geoconvention
Virtual Event
September 13 - 15
2021

Semi-continuous Electrical Resistivity Tomography monitoring for CO2 injection at the CaMI Field Research Station, Newell County, Alberta, Canada

Marie Macquet[1], Don C. Lawton[1,2], Dennis Rippe[3] and Cornelia Schmidt-Hattenberger[3]

[1] Carbon Canada Management (CMC), [2] University of Calgary, [3] GFZ German Research Centre for Geosciences

Summary

CMC's CaMI Field Research hosts a broad range of geophysical and geochemical instruments used to quantify the detection threshold for different monitoring technologies for CO_2 injected and stored in the subsurface. In this paper, we show results from the borehole-borehole Electrical Resistivity Tomography (ERT) method. We present the method and the dataset, the time-lapse inversion results, and the future work. The raw data shows a good correlation between resistivity index (ratio between baseline resistivity and monitor resistivity) and the CO_2 injection history. The inversion results show two zones with resistivity increase: at 300 m depth (corresponding to the injection zone) and at 280 m depth (corresponding to a coal zone). The CO_2 saturation estimated from the inverted resistivity models is in good correlation with the CO_2 reservoir modelling. Between the two high-resistivity zones is a zone where the resistivity decreases. A full comprehensive analysis of the system complexity (CO_2 injection, dissolution, geochemical processes, CO_2 migration) and their impacts on the resistivity are still being addressed to fully understand these results.

Introduction

At CaMI.FRS, 128 electrodes are permanently installed, with 116 electrodes at a 10 m spacing buried at 1m depth along the 1.1 km trench, and 16 electrodes in a monitoring well 20 m SW of the injection well. The borehole electrodes are located every 5 m between depths of 245 and 320 m, covering the injection layer (295 to 302m depth). Electrical Resistivity Tomography (ERT) is a useful geophysical tool to estimate the CO_2 saturation because of the ERT high sensitivity to the presence and the composition of pore fluids. The method is well developed for near-surface imaging (e.g., Binley and Kemna, 2005; Loke et al.,2013), and due to the high resistivity of injected CO_2 as comparison with the in-place brine, the method is extremely valuable for CO_2 injection and storage monitoring. Few sites are studying the possibilities of such complementary geophysical methods (ERT/EM), as shown at Cranfield, Mississippi, US (Carrigan et al., 2013), Nagoaka, Japan (Mito and Xue., 2011), Hontomín, Spain (Vilamajó et al., 2013) and Ketzin, Germany (Schmidt-Hattenberger et al., 2011; Bergmann et al., 2017). The CaMI.FRS differs from the other sites because of the very small volume of injected CO_2 (33.8 tonnes end of February 2021) and only one monitoring well is equipped with electrodes. Figure 1b shows the lithology of the zone covered by the electrodes, as well as the associated resistivity extracted from well logs.

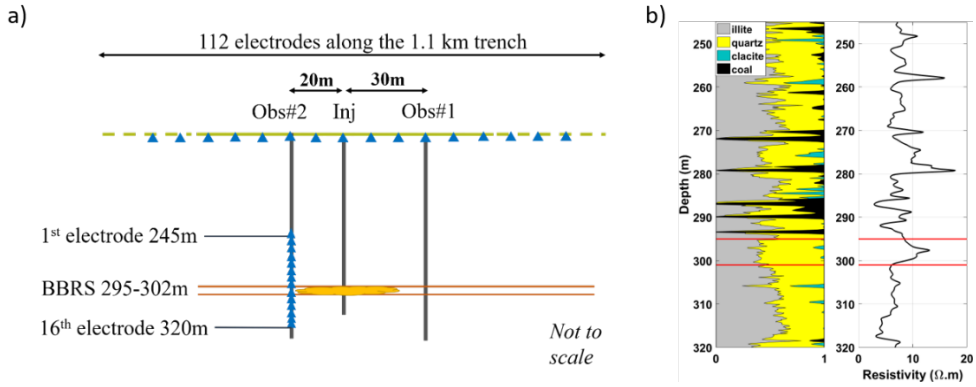

Figure 1: a) Schematic of the ERT installation at the CaMI.FRS. b) CaMI.FRS lithology and resistivity extracted from well log, zoomed in the zone of interest. Red lines delimit the Basal Belly River Sandstones (BBRS) which is the injection zone.

Theory

The ERT method applied to fluid composition estimation is based on Archie's law (1942):

$$\rho = a.\emptyset^{-m}.S_w^{-n}.\rho_w \quad (1)$$

where ρ is the composite resistivity of the rock, ρ_w is the resistivity of the brine, S_w is the saturation of the brine, $\emptyset$ is the porosity of the rock, m is the cementation factor of the rock, n is the saturation exponent and a is the proportionality constant. m, n, and a are assumed or determined empirically using laboratory analysis. Potential errors on rock parameters (especially m, $\emptyset$ and a) can induce significant uncertainties in the resistivity predicted by a model (Bergmann et al., 2017). To overcome this problem, we use Guéguen and Palciauskas (1994) equation:

$$RI = \frac{R}{R_0} = (S_w)^{-n} \quad (2)$$

where R_0 is the baseline resistivity and R is the monitor resistivity. RI is the resistivity index (or resistivity ratio). Thus, the only estimated empirical constant is n the saturation exponent. We used n = 2 in this study. CO_2 saturation (S_{CO_2}) is estimated using:

$$S_{CO_2} = 1 - S_w = 1 - \left(\frac{1}{RI}\right)^{1/n} \quad (3)$$

Dataset

In this paper, we are using the data obtained using borehole-borehole configurations. Because they are less sensitive to the small amount of CO_2 injected at 300 m depth, the data obtained using the surface electrodes are part of a future work. We started almost daily surveys using the 16 borehole electrodes on September 18th 2019. We missed few surveys due to equipment failure, in particularly toward the end of 2019. We built our baseline dataset using the average of 10 surveys (Sept. 18th to Sept. 30th, 2019) to be sure to exclude errors due to possible outliers in our baseline.

Figure 2 shows the raw resistivity ratio (R/R_0) evolution, using the average of the last 10 days of September 2019 as baseline resistivity. Depending on the electrodes used for the measurement, the pseudo-depth and pseudo-distance can be estimated. Figure 2 shows times series of the resistivity ratio, sampling different distances from the observation well. Since CO_2 has a higher resistivity compared to the brine, an increase of the ratio can be attributed to the injected CO_2 replacing the brine in the pore spaces.

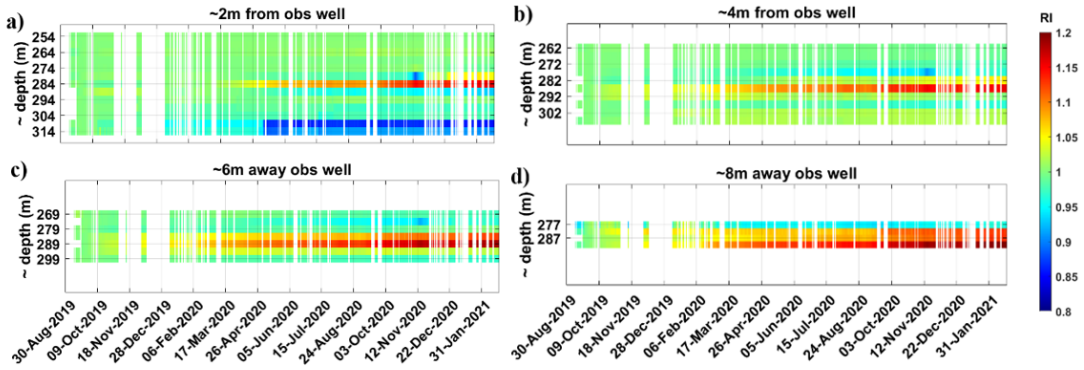

Figure 1: Resistivity ratio (RI) for dipole-dipole configurations, for different distances from the observation well. Baseline resistivity is the average from Sept. 18th to Sept. 30th 2019. a) are the configurations sensitive to 2 m around the observation well; ; b) 4 m around obs. well; c) 6 m around obs. well; d) 8 m around obs. well. The further from the observation well, the closer from the injection well.

We notice in Figure 2 the following:

- The resistivity increases earlier in time when we get further from the observation well, meaning that we observe the CO_2 effect first close to the injection well. We can see the effect of CO_2 injection as early as October 2019 when we are 8 m away from the observation well (Figure 2d), whereas effect is noticeable only in March 2020 when we are 2 m away from the observation well (Figure 2a).

- The resistivity increase is more obvious when we are closer to the injection well (Figure 2d), which is interpreted to be due to a higher CO_2 saturation near the injector well.

Careful analysis of the reciprocal errors (for reliability of the measurement) and the contact resistances (health of the electrodes) was done to make sure that the evolution of the observed resistivity is due to change in the medium and not due to any degradation of the electrodes.

Inversion

If the time series gives a good first approximation, attributing a single spatial point to a measurement do not reflect the full complexity of ERT measurement sensitivity kernel. We use the Python R2 codes package (Binley, 2020) to perform the inversion. As mentioned earlier, we used only the borehole-borehole surveys. The measurement configuration was dipole-dipole and data showing a reciprocal error > 15% were excluded from the inversion.

We average 10 daily surveys (from September 19th to September 30th 2019) to get the baseline model. Averaging 10 surveys allows to reduce the risk of outlier measurements. We use a homogeneous starting model, with a resistivity of 7 $\Omega.m$ (based on the well log. Figure 1). We use a maximum of 10 iterations and stop the inversion once we reach an RMS of 1. The inverted baseline is used as starting model for each monitor survey inversion.

Figure 3 (a-d) shows different resistivity ratio time-lapse between the baseline and different monitor surveys. We observe resistivity anomalies building up with time in 2 zones:

- At 300 m depth which is the injection target.
- At 280 m depth which is a coal layer of high baseline resistivity (see Figure 1).

Between these high resistivity anomalous zones, the resistivity is observed to decrease with respect to the baseline model, but this could be an artifact of the inversion. If we consider that the increase of resistivity is due only to CO_2 replacing the brine, we obtain Figure 2(e-h) using equation 3.

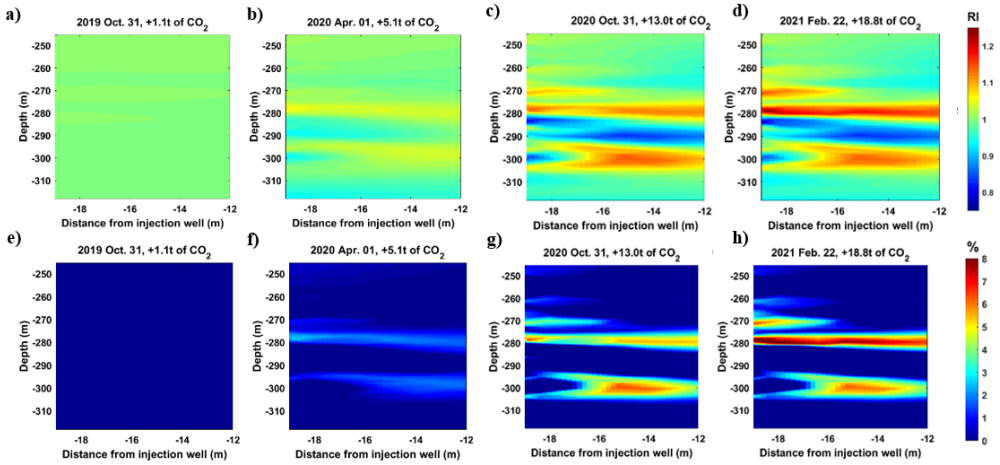

Figure 3: a-d) Resistivity ratio (RI) between the baseline (Sept. 2019) and subsequent monitor surveys. e-h) Corresponding CO_2 saturation (%) obtained from the resistivity ratio and equation 3. Note that already 15 tonnes of CO_2 were already injected in September 2019.

We observe in Figure 3 (e-f) that the reservoir (300 m depth) is becoming saturated with injected CO_2. Quite quickly in time, the layer at 280 m depth also starts to show an increase in resistivity (Figure 3.b) that we attribute to CO_2 accumulation. However, more complex processes may be taking place here such as methane production from the coal layer. Produced gases at the monitoring well have been sampled and will be analyzed to help us understand the complex interconnected processes that are happening above the injection zone.

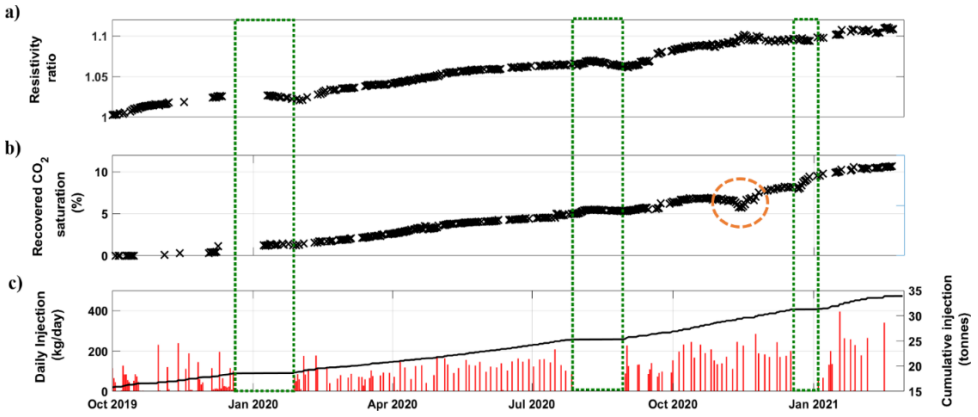

Figure 4: a) Raw resistivity ratio (from Figure 2) for ~300m depth. b) CO2 saturation recovered from resistivity inversion (from Figure 3 (e-h)). c) CO2 injection history (daily and cumulative). Green boxes highlight the different times where the injection stopped. The orange circle is due to ERT power supply failure during this period.

Figure 4 compares the raw resistivity ratio, the CO_2 saturation recovered from the inversion process and using equation 3, and the injection history at the CaMI Field Research Station. The three different variables show a very good correlation. We observe a slight decrease in the resistivity ratio and a stagnation in the CO_2 saturation during the periods where the injection was stopped. The decrease of CO_2 saturation mid-November 2020 is attributed to a failure of the FRS ERT power supply inducing errors in the observed resistivity data. A large decrease in resistivity can be observed during this period (Figure 2).

Conclusions

Error analysis is crucial when reviewing the raw data, especially when looking at small changes in the resistivity ratio. One might easily interpret a change of resistivity as a change in the subsurface while it could be due to an increase in errors on the measurements or a power supply issue. By careful quality control of the raw data, we obtain a reliable interpretation that the changes in measured resistivity are directly correlated to the CO_2 injection. Inversion process gives spatial maps of theses changes, and the CO_2 saturation obtained from the inverted resistivity models shows a good correlation with the CO_2 injection. The saturation obtained is coherent with our injection numerical simulation.

Surface electrodes are not included in this study because they are less sensitive to the small amount (33.8 tonnes so far) of injected CO_2 at 300m depth than the borehole electrodes. As the volume of injected gas increases, we will include them in the inversion. The surface-surface configurations will not provide detailed resistivity images at the injection depth but will provide effective monitoring for any CO_2 that might migrate upwards out of the injection zone. Surface-borehole configurations will also help constrain the inversion. A sensitivity analysis is required to select the optimum schedule as using the full 128 electrodes can provide more than 250 million different electrode configurations.

The CaMI Field Research is one in-a-kind site, bridging the gap between large scale CO_2 storage sites and laboratory experiments. We are facing complex geochemical reactions including gas

production at the observation well, possible hydrate formation due to the pressure/temperature conditions at 300 m depth making the interpretation of the resistivity models very interesting.

Acknowledgements

We thank the CaMI.FRS JIP members for their support for this project. The authors also acknowledge financial support from the University of Calgary's Canada First Research Excellence Fund program: the Global Research Initiative in Sustainable Low-Carbon Unconventional Resources, and the CREWES project at the University of Calgary. We thank Malcolm Bertram for his valuable help on the field.

References

Archie, G. E., 1942, The electrical resistivity log as an aid in determining some reservoir characteristics: Transactions of the AIME, 146, No. 01, 54–62, doi:10.2118/942054-G.

Bergmann, P., Schmidt-Hattenberger, C., Labitzke, T., Wagner, F. M., Just, A., Flechsig, C., and Rippe, D., 2017, Fluid injection monitoring using electrical resistivity tomography—five years of CO_2 injection at Ketzin, Germany: Geophysical Prospecting, 65, No. 3, 859–875, doi:10.1111/1365-2478.12426.

Binley, A., 2020, R2 - free resistivity software - http://www.es.lancs.ac.uk/people/amb/Freeware/R2/R2.htm (accessed November 23 2020): WWW document.

Binley, A., and Kemna, A., 2005, DC resistivity and induced polarization methods, in Hydrogeophysics, Springer, 129–156

Carrigan, C. R., Yang, X., LaBrecque, D. J., Larsen, D., Freeman, D., Ramirez, A. L., Daily, W., Aines, R., Newmark, R., Friedmann, J. et al., 2013, Electrical resistance tomographic monitoring of CO_2 movement in deep geologic reservoirs: International Journal of Greenhouse Gas Control, 18, 401–408, doi:10.1016/j.ijggc.2013.04.016.

Guéguen, Y., and Palciauskas, V., 1994, Introduction to the Physics of Rocks: Princeton University Press.

Lawton, D.C., Osadetz, K. & Saeedfar, A. 2017. CCS monitoring technology innovation at the CaMI field research station, Alberta, Canada. *EAGE/SEG Research Workshop 2017, Geophysical Monitoring of CO_2 Injection: CCS and CO_2-EOR, Trondheim, Norway, August 2017*, doi:10.3997/2214-4609.201701930.

Lawton D. C., Dongas J., Osadetz K., Saeedfar A. & Macquet M. 2019. Development and Analysis of a Geostatic Model for Shallow CO_2 Injection at the Field Research Station, Southern Alberta, Canada. Chapter 16 in *Geophysics and Geosequestration*, Cambridge University Press, Editors: Thomas L. Davis, Martin Landro, Malcolm Wilson.

Loke, M., Chambers, J., Rucker, D., Kuras, O., and Wilkinson, P., 2013, Recent developments in the direct current geoelectrical imaging method: Journal of applied geophysics, 95, 135–156, doi:10.1016/j.jappgeo.2013.02.017.

Macquet, M., Lawton, D. C., Saeedfar, A., and Osadetz, K. G., 2019, A feasibility study for detection threshold of CO_2 at shallow depths at the CaMI Field Research Station, Newell County, Alberta, Canada: Petroleum Geoscience, 24, no. 5, 509-518doi:10.1144/petgeo2018-135.

Mito, S and Xue Z., 2011, Post-Injection Monitoring of Stored CO2 at the Nagaoka Pilot Site: 5 Years Time-Lapse Well Logging Results, Energy Procedia, 4, 3284-3289, doi:10.1016/j.egypro.2011.02.248

Schmidt-Hattenberger, C., Bergmann, P., Labitzke, T., Schröder, S., Krüger, K., Rücker, C., and Schütt, H., 2011, Monitoring of geological CO_2 storage with electrical resistivity tomography, Berichte Geol. B.-A, 93, 75-81.

Vilamajó, E., Queralt, P., Ledo, J., and Marcuello, A., 2013, Feasibility of monitoring the Hontomín (Burgos, Spain) CO_2 storage site using a deep EM source: Surveys in Geophysics, 34, no. 4, 441–461.